SCIENCE AND TECHNOLOGY ORGANIZATION
CENTRE FOR MARITIME RESEARCH AND EXPERIMENTATION

Reprint Series **CMRE-PR-2014-011**

A novel approach for a bistatic scattering calculation suitable for sonar performance model

Gaetano Canepa, Alessandra Tesei

January 2014

Originally published in:

Proceedings of the 11th European Conference on Underwater Acoustics, Edinburgh, July 2012.

Proceedings of Meetings on Acoustics, Vol. 17, 070096 (2013).

About CMRE

The Centre for Maritime Research and Experimentation (CMRE) is a world-class NATO scientific research and experimentation facility located in La Spezia, Italy.

The CMRE was established by the North Atlantic Council on 1 July 2012 as part of the NATO Science & Technology Organization. The CMRE and its predecessors have served NATO for over 50 years as the SACLANT Anti-Submarine Warfare Centre, SACLANT Undersea Research Centre, NATO Undersea Research Centre (NURC) and now as part of the Science & Technology Organization.

CMRE conducts state-of-the-art scientific research and experimentation ranging from concept development to prototype demonstration in an operational environment and has produced leaders in ocean science, modelling and simulation, acoustics and other disciplines, as well as producing critical results and understanding that have been built into the operational concepts of NATO and the nations.

CMRE conducts hands-on scientific and engineering research for the direct benefit of its NATO Customers. It operates two research vessels that enable science and technology solutions to be explored and exploited at sea. The largest of these vessels, the NRV Alliance, is a global class vessel that is acoustically extremely quiet.

CMRE is a leading example of enabling nations to work more effectively and efficiently together by prioritizing national needs, focusing on research and technology challenges, both in and out of the maritime environment, through the collective Power of its world-class scientists, engineers, and specialized laboratories in collaboration with the many partners in and out of the scientific domain.

NOTE: The CMRE Reprint series reprints papers and articles published by CMRE authors in the open literature as an effort to widely disseminate CMRE products. Users are encouraged to cite the original article where possible.

Proceedings of Meetings on Acoustics

Volume 17, 2012 http://acousticalsociety.org/

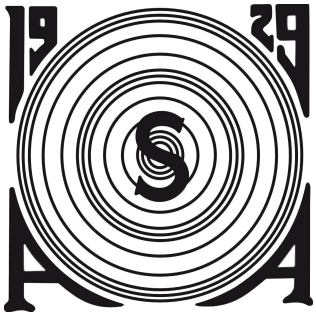

ECUA 2012 11th European Conference on Underwater Acoustics
Edinburgh, Scotland
2 - 6 July 2012

Session UW: Underwater Acoustics

UW246. A novel approach for a bistatic scattering calculation suitable for sonar performance model

Gaetano Canepa* and Alessandra Tesei

***Corresponding author's address: Center for Maritime Research and Experimentation, La Spezia, Italy, canepa@cmre.nato.int**

One of the classical approaches to the calculation of the sound pressure scattered from a rough surface is to sum the contributions to the field from a set of small tiles that approximate the surface. If the tiles are smaller than the wavelength, or infinitesimal, the Kirchhoff's, the Small slope and small perturbation approximations can give good results. However, these approximations are computational intensive. In addition, if the tiles are larger than the wavelength these approximations cannot be applied. This work proposes a novel approach to accurately calculate the bistatic scattering from a rough surface approximated by tiles larger than the wavelength. The theory behind the calculations includes both specular and off-specular scattering components with their correct amplitude contributions. The results of the new approach are applied to a sonar performance model and compared with high frequency data. The model-data comparison demonstrates the validity of the theory.

Published by the Acoustical Society of America through the American Institute of Physics

 [DOI: 10.1121/1.4802974]
Received 26 Nov 2012; published 15 Apr 2013
Proceedings of Meetings on Acoustics, Vol. 17, 070096 (2013)

1 INTRODUCTION

By paying attention to Sonar Performance (SP) one would expect the optimal planning of a sidescan or Synthetic Aperture Sonare (SAS) to result in reduction of execution time (with important economic benefits) and in data quality improvement. The sonar performance depends on many parameters: sonar frequency, receiving and transmitting beam patterns, seafloor geophysical features and bathymetry, sea surface conditions and oceanographic conditions (such as sound speed profile, *etc.*). PAR-TIME, a model of SP that produces realistic results taking into account all these variables, has been under investigation for several years at STO-CMRE (former NATO Underwater Research Centre, NURC) [1]. A factor limiting the development of such a model is the lack of high-frequency forward and backward acoustic scattering data acquired along with accurate, independent measurements of the parameters that affect SP. In particular, sound propagation data including higher-order multipaths at high-frequency are rare and not well characterized.

In 2009 NURC conducted the MARES sea campaign, the purpose of which was to collect high-frequency (300 kHz) scattering data in very shallow water. The configuration of the experiment was chosen to ensure the presence of higher order multipaths [2–4]. Some features outlined in the at-sea data could not be predicted by available scattering models, and a new approach (implemented in the PAR-TIME model) was proposed at that time [1], which was able to explain some of the data characteristics and properly simulate forward scattering. So far PAR-TIME model results have been compared only to forward scattering data for two reasons:

- forward scattering data acquired during MARES are calibrated and extremely well characterized, and
- the backscattering model can give correct results only if the forward scattering model is accurate because the forward scattering is the easier to approximate by many scattering models, and the backscattering model includes echo from multipath (essentially caused by backscattering from boundaries insonified by forward scattering).

In the last two years PAR-TIME has been further developed, and in the meantime more discrepancies between forward scattering at-sea and simulated data have been discovered. The reason for these discrepancies can be explained once the geometry and configuration of the experiment has been described (Figure 1). At the top of Figure 1 the experimental geometry which was used to acquire forward scattering data is shown: the transmitter is a Neptune Sonar Limited T36 sidescan transducer mounted in such a way as to use the narrow part of the beam (one degree beam width) to insonify the boundaries of the sound channel, while the wide part of the beam is perpendicular to the figure plane. The experiment consisted of repeatedly emitting a ping by pointing the transducer in such a way as to selectively excite the most significant multipaths from transmitter to receiver (shown in the figure as paths A to F). The very narrow beam of the transducer was supposed to allow accurate high resolution in multipath selection. The receiver (RX) is an array of three omnidirectional transducers. The acquisitions from the central transducer are shown in the bottom part of Figure 1. The transmitted signal is a Linear Phase Modulation (LPM) pulse with a 60 kHz bandwidth centered around 300 kHz. The length of the pulse was 1 ms and the data shown in the figure are matched filtered. The

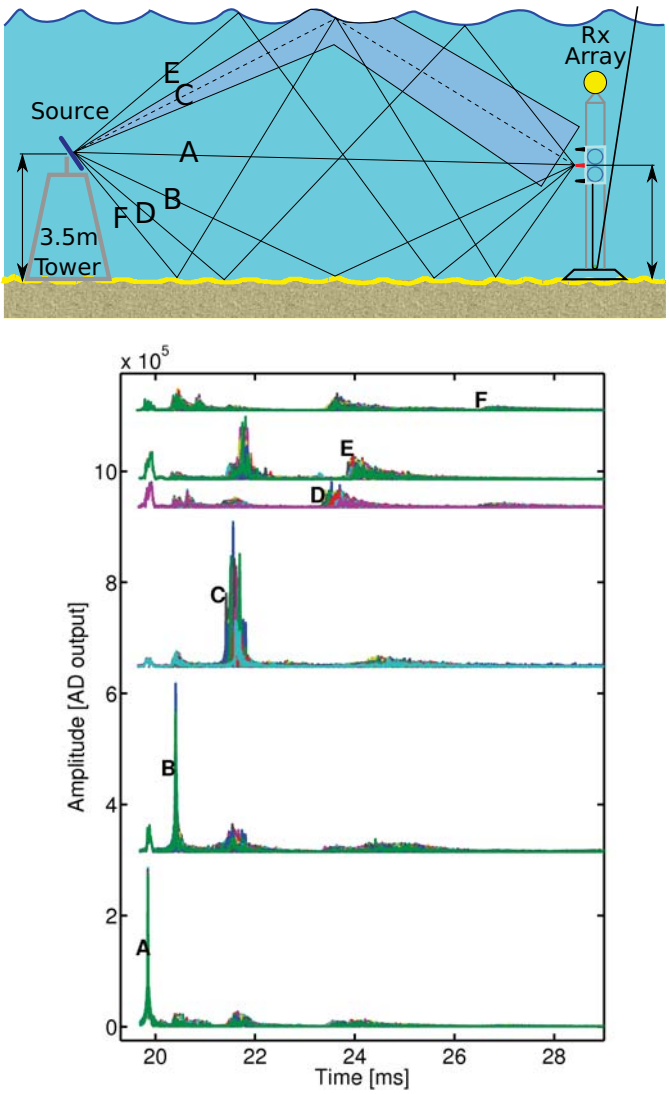

Figure 1: Top: experimental geometry. The selected paths between source and receiver are tagged A to F. The corresponding arrival echoes are shown in the lower plots. They show the envelope of the arrivals which are shifted in amplitude in order to enhance readability. Here and in the following figures the linear scale is used to enhance the arrival variability.

bottom part of Figure 1 shows, overlapped in different colours, all 80 pings received when the source transducer was directed at different angles (from A to F). The amplitude of the B to F arrivals is to be compared to that of the direct arrival (A). It can be observed that some of the arrivals including bounces from the boundaries are higher than the direct arrival (A) even if the travel length is longer and some loss is expected. If an amplitude average is performed on the scattered arrivals, *e.g.*, in the case of the sea-surface scattering arrivals, the average is attenuated with respect to the theoretical reflected echo by about 35% [5]. Data in Figure 1 also show the presence of non-specular arrivals (sometimes of large amplitude with respect to the specular one) and of sidelobe arrivals. This cannot be easily explained with current SP models that only consider specular reflections in the forward direction. In the following section an interpretation of the differences between at-sea and simulated data is provided. In Section 3 a theoretical solution that can remove the discrepancies is given. The last section will show the simulation results that can be achieved after the theoretical solution proposed in Section 3 is implemented into PAR-TIME.

2 MODEL-DATA COMPARISON

The fundamental idea at the basis of the PAR-TIME model consists of dividing the sea surface and the bottom in facets that are large with respect to the sound wavelength (between 0.25 and 0.5 m with respect to 5e-3 m). The eigenrays from the source to each facet (on the surface and on the bottom) and from each facet to the receiver are computed with the help of an iterative algorithm that uses a ray-tracer [6]. The arrival echo is calculated adding the contribution from each facet considering the source beam pattern, the eigenrays travel path and travel time, and a scattering model characteristic to PAR-TIME [1]. The problem is how to properly combine all these elements. This is a problem common to most high frequency sonar performance models, independently on which specific scattering model they use.

Focusing only on the first three arrivals in Figure 1 (A, B and C), a puzzling discrepancy forced us to modify PAR-TIME on the basis of a theoretical development which is described in this work. If the size of the facet is much smaller than the sound wavelength, the Kirchhoff approximation can be used, and the contribution of a facet can be computed as inversely proportional to the product of R_{i0} times R_{r0}, where R_{i0} is the distance between source and facet, and R_{r0} is the distance between facet and receiver. If such a rule is applied to the computation of the contribution to the arrival, the simulation results are as in the left side of Figure 2. From this figure it is easy to verify that the arrival times are correct, but the scattering amplitudes are much lower than in the experimental data (see Figure 1). If the same sound channel is simulated using the model BORIS-SSA (set for first order small slope approximation) and the appropriate facet size (0.5 mm), the correct amplitude and statistics of the sound arrival is obtained [2, 3].

In forward scattering many models use the approximation of pure reflection from the boundary, even if the presence of non specular arrivals in Fig. 1 (see arrivals on curves D and E at 20.5 and 21.7 ms respectively[1]) suggest that pure reflection is not a good choice. On the other hand it is known that when one looks exactly in the specular direction, the presence of roughness on the scattering surface does not influence very much the reflected amplitude (for small roughness amplitude and slope). Hence, the sound scattered outside the reflection direction is a small fraction of the reflected one. If the equation to compute the facet contribution to the arrivals is inversely proportional to the sum of R_{i0} plus R_{r0} (a "reflection-like" compromise), the modeling tool provides the plot on the right of Figure 2. The arrivals in this figure are now closer in amplitude to the direct arrival but their shapes are wider than the experimental ones (in the case of sea surface arrivals). Moreover, the plot shows, after the first arrival peak, one or two peaks that are not present in the data. In summary:

- when the receiver is exactly in the reflection position, the reflection equation gives good results;
- when the receiver if FAR from the reflection angle, the scattering equation is expected to be more adequate;
- what FAR means and how the two equations are interpolated is the subject of this work.

3 THEORETICAL APPROACH

In this section we show how an equation satisfying the above criteria can be computed theoretically. Following Clay and Medwin [7] with minimal differences, we start from the Helmholtz-Kirchhoff integral:

$$p(\mathbf{R_{i0}}, \mathbf{R_{r0}}) = \frac{1}{4\pi} \int_S \left[p \frac{\partial \psi}{\partial n} - \psi \frac{\partial p}{\partial n} \right] ds, \tag{1}$$

where $p(\mathbf{R_{i0}}, \mathbf{R_{r0}})$ is the total sound pressure at $\mathbf{R_{r0}}$ caused by a source in $\mathbf{R_{i0}}$ and p is the sound pressure on the surface,

$$\psi = \frac{e^{ik_0 R_r}}{R_r}, \tag{2}$$

[1] These are non-specular arrivals from the first bounces of the sound beams from the boundary.

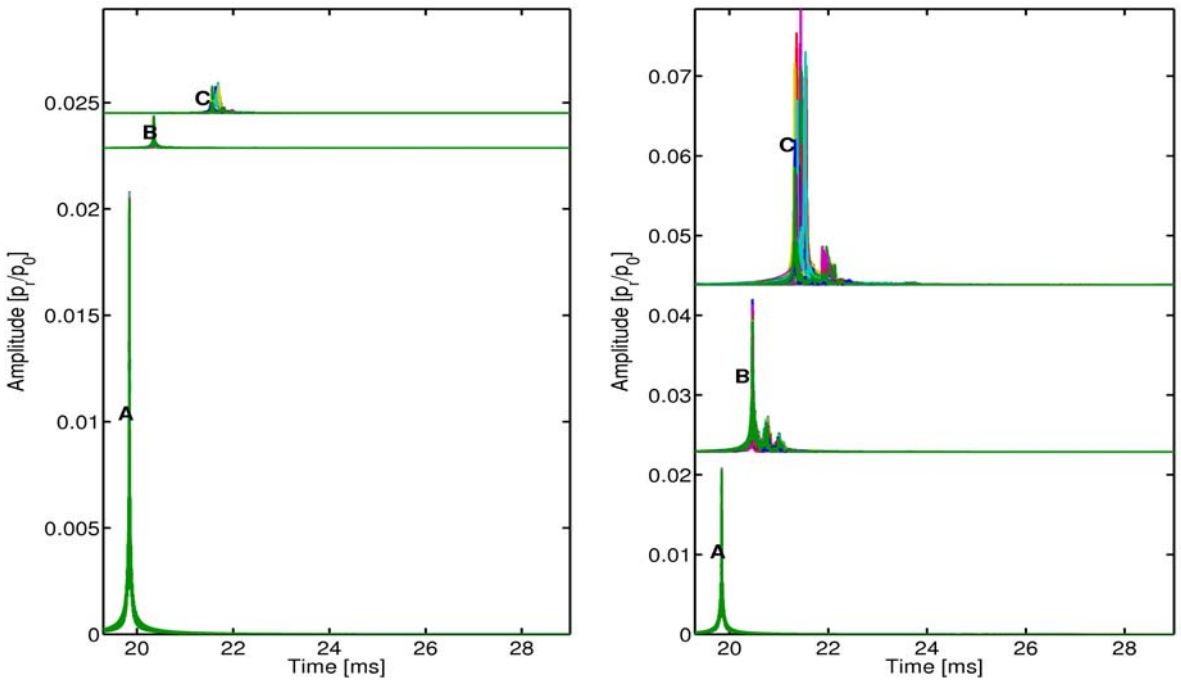

Figure 2: Left plot: simulation results for path A to C if scattering-like contribution from each facet is used ($\propto \frac{1}{R_{i0}R_{r0}}$). Right plot: simulation results if a specular-like contribution is used ($\propto \frac{1}{R_{i0}+R_{r0}}$).

and R_r is the distance between the infinitesimal area ds and the receiver, k_0 the water wave number ($k_0 = 2\pi/\lambda$), λ the wavelength ($\lambda = c_0/f$), c_0 the wave sound speed and f the source sound frequency. We suppose that the incident pressure is a spherical pressure field with a Gaussian beam pattern,

$$p_i = p_0 \frac{e^{ik_0 R_i}}{R_i} e^{\frac{-x^2}{2L^2}}, \tag{3}$$

where R_i is the distance between the source and ds, p_0 is the source pressure amplitude, L define the beam amplitude and x is defined in Figure 3. The Gaussian beam approximation is not necessary as the result given here only depends on the vanishing of the sound pressure outside the facet along the x direction. A different approximation (see [8, 9]) could be achieved by considering every single facet isolated in space and constant insonification. The resulting equation is only marginally different from what we obtained here except for the presence of side-lobes in the final results. The beam pattern in Equation (3) is constant along y: in this way the results of this work can be applied to 2D problems.

For angles close to the specular direction and for small slope and height of the roughness profile, it is possible to use the Kirchhoff approximation for p_s, the scattered wave field from the surface [7]:

$$p_s = V(\theta_i) p_i = p_0 V(\theta_i) \frac{e^{ik_0 R_i}}{R_i} e^{\frac{-x^2}{2L^2}}, \tag{4}$$

where $V(\theta_i)$ is the plane wave reflection coefficient calculated for each point $(x, z) \in S$ and p_i is the incident pressure field from a point source. The equation adopted here will be accurate only when the Kirchhoff approximation holds. If only the scattered sound in the far field is considered ($k_0 R_i \gg 1$ and $k_0 R_r \gg 1$), and if $L k_0 \cos\theta_i \gg 1$ (high frequency, non-vanishing grazing angle, wide beam pattern) and supposing $\frac{\partial V(\theta_i)}{\partial n} \approx 0$ we have

$$\frac{\partial \psi}{\partial n} = i \frac{\mathbf{R_{r0}}}{R_{r0}} \cdot \mathbf{n} k_0 \frac{e^{ik_0 R_r}}{R_r} = i \cos\theta_r k_0 \frac{e^{ik_0 R_r}}{R_r}, \text{ and} \tag{5}$$

$$\frac{\partial p}{\partial n} = -ip_0 \frac{\mathbf{R_i}}{R_i} \cdot \mathbf{n} V(\theta_i) k_0 \frac{e^{ik_0 R_i}}{R_i} = -ip_0 \cos\theta_i V(\theta_i) k_0 \frac{e^{ik_0 R_i}}{R_i} e^{\frac{-x^2}{2L^2}}, \tag{6}$$

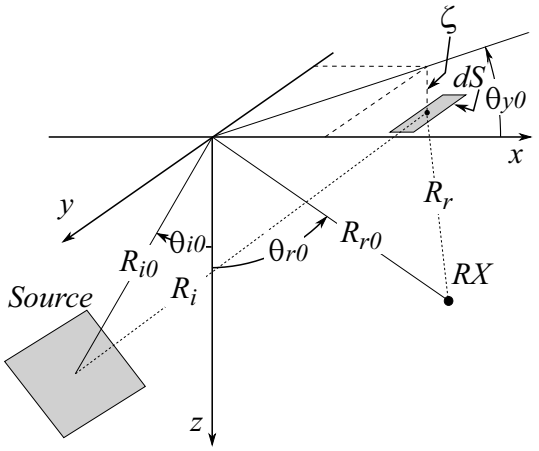

Figure 3: Geometry: dS is at position x, y, ζ relative to the intersection between the scattering surface and the center of the source beam pattern assumed as origin (adapted from [7]).

where $\cos\theta_i$ and $\cos\theta_r$ depend on the point $(x, z) \in S$ considered. Substituting equations (4)–(6) in (1) and considering only the scattered pressure, we obtain

$$p_s(\mathbf{R_i}, \mathbf{R_r}) = \frac{ik_0 p_0}{4\pi} \int_S V(\theta_i) \left(\cos\theta_r + \cos\theta_i\right) \frac{e^{ik_0(R_i+R_r)}}{R_i R_r} e^{\frac{-x^2}{2L^2}} ds. \tag{7}$$

A particular form of this equation (for a plane wave source incident on a finite facet of surface) was considered in Bekmann and Spizzichino [8]. Starting from that equation, they define the scattering coefficient $\rho(\mathbf{R_r})$ as the ratio between the (coherent and incoherent) scattered pressure at $\mathbf{R_r}$ and the pressure reflected by a smooth pressure release surface of the same size. They found that the average scattering coefficient for a rough surface follows the relation

$$\langle \rho(\mathbf{R_r}) \rangle = \chi(k_0(\sin\theta_i - \sin\theta_r)) \rho_0(\mathbf{R_r}), \tag{8}$$

where $\rho_0(\mathbf{R_r})$ is the scattering coefficient of a smooth surface and χ is the characteristic function associated with the distribution $w(z)$ of the rough surface height,

$$\chi(\sin\theta_i - \sin\theta_r) = \int_{-\infty}^{\infty} w(z) e^{i(\sin\theta_i - \sin\theta_r)z} dz = \langle e^{i(\sin\theta_i - \sin\theta_r)\zeta} \rangle. \tag{9}$$

Our aim is to find the same relation (8) for a spherical wave as given in equation (7). The influence of the roughness can be applied to any SP model, depending on how it deals with scattering. In the following, without loss of generality and for simplicity, a pressure release surface ($V(\theta_i) = -1$) is considered[2]. As in [8], a smooth surface is taken where $\rho_0(\mathbf{R_i}, \mathbf{R_r})$ is defined as the ratio between the reflected pressure at $\mathbf{R_r}$ ($p(\mathbf{R_r})$) and the pressure reflected by a smooth pressure release surface of the same size ($p_0(\mathbf{R_r})$). Since a smooth surface is used to develop the following, the Kirchhoff approximation holds. Equation (7) becomes:

$$p_s(\mathbf{R_i}, \mathbf{R_r}) = -\frac{ik_0 p_0}{4\pi} \iint_{-\infty}^{\infty} \left(\cos\theta_r + \cos\theta_i\right) \frac{e^{ik_0(R_i+R_r)}}{R_i R_r} e^{\frac{-x^2}{2L^2}} dx dy. \tag{10}$$

In order to find the value of $p_s(\mathbf{R_i}, \mathbf{R_r})$ near specular reflection, the first order approximation of R_i, R_r, $R_i + R_r$ and $R_i R_r$ is computed for $\zeta = 0$ and under the far field condition (as above):

$$L \gg \lambda,\ R_{i0} \gg L \text{ and } R_{r0} \gg L.$$

Using the conventions from Figure 3, Clay and Medwin [7] give for $R_i + R_r$ and $R_i R_r$:

$$\begin{aligned} R_i + R_r &= R_{i0} + R_{r0} + \alpha x + \beta y + U_x x^2 + U_y y^2, \\ R_i R_r &= R_{i0} R_{r0} + \gamma x + \eta y. \end{aligned}$$

[2]The assumption is a constant or slow varying Reflection Coefficient in the insonified area.

with

$$\begin{aligned}
\alpha &= \sin\theta_{i0} - \sin\theta_{r0}\cos\theta_{y0},\\
\beta &= \sin\theta_{i0}\sin\theta_{y0},\\
\gamma &= R_{r0}\sin\theta_{i0} - R_{i0}\sin\theta_{r0},\\
\eta &= R_{i0}\sin\theta_{r0}\sin\theta_{y0},\\
U_x &= \frac{1}{2}\left(\frac{1-\sin^2\theta_{r0}\cos^2\theta_{y0}}{R_{r0}} + \frac{\cos^2\theta_{i0}}{R_{i0}}\right),\\
U_y &= \frac{1}{2}\left(\frac{1-\sin^2\theta_{r0}\sin^2\theta_{y0}}{R_{r0}} + \frac{1}{R_{i0}}\right).
\end{aligned}$$

In the specular reflection region

$$\beta = 0,\ \eta = 0,\ \theta_{y0} = 0,\ U_x = \frac{1}{2}\left(\frac{\cos^2\theta_{r0}}{R_{r0}} + \frac{\cos^2\theta_{i0}}{R_{i0}}\right),\ U_y = \frac{1}{2}\left(\frac{1}{R_{r0}} + \frac{1}{R_{i0}}\right), \tag{11}$$

and the integral in equation (10) becomes

$$p(\mathbf{R_i}, \mathbf{R_r}) = -\frac{ik_0 p_0}{4\pi}\iint_{-\infty}^{\infty}(\cos\theta_r + \cos\theta_i)\,\frac{e^{ik_0\left(R_{i0}+R_{r0}+\alpha x+U_x x^2+U_y y^2\right)}}{R_{i0}R_{r0}+\gamma x}e^{\frac{-x^2}{2L^2}}\,dxdy. \tag{12}$$

This integral can be evaluated using the method of stationary phase. From Born and Wolf [10] a double integral of the form

$$\phi = \iint g(x,y)e^{ik_0 f(x,y)}dxdy \tag{13}$$

can be evaluated in the region where g(x,y) changes slowly and

$$\frac{\partial f}{\partial x} = \frac{\partial f}{\partial y} = 0. \tag{14}$$

For a large value of the real part of k_0 (high frequency), the integral (13) tends asymptotically to the value given by

$$\phi = \frac{i2\pi\sigma}{k_0\sqrt{|ab-c^2|}}g(x_0,y_0)e^{ik_0 f(x_0,y_0)}, \tag{15}$$

where x_0 and y_0 are the roots of equations (14), and

$$a = \left.\frac{\partial^2 f}{\partial^2 x}\right|_{x_0},\quad b = \left.\frac{\partial^2 f}{\partial^2 y}\right|_{y_0},\quad c = \left.\frac{\partial^2 f}{\partial x\partial y}\right|_{x_0,y_0},$$

$$\sigma = \begin{cases} 1 & \text{for } ab > c^2 \text{ and } a > 0\\ -1 & \text{for } ab > c^2 \text{ and } a < 0\\ -1 & \text{for } ab < c^2. \end{cases} \tag{16}$$

In our case we have

$$\begin{aligned}
a &= 2U_x,\\
b &= 2U_y,\\
c &= 0,\\
\frac{\partial f}{\partial x} &= \alpha + 2U_x x = 0 \Rightarrow x_0 = -\frac{\alpha}{2U_x},\\
\frac{\partial f}{\partial y} &= 2U_y y = 0 \Rightarrow y_0 = 0,\\
\sigma &= 1,\\
g(x_0,y_0) &= (\cos\theta_{r0} + \cos\theta_{i0})\,\frac{e^{ik_0(R_{i0}+R_{r0})}e^{\frac{-x_0^2}{2L^2}}}{R_{i0}R_{r0}+\gamma x_0},\ \text{and}\\
f &= \alpha x_0 + U_x x_0^2 = -\frac{\alpha^2}{4U_x},
\end{aligned}$$

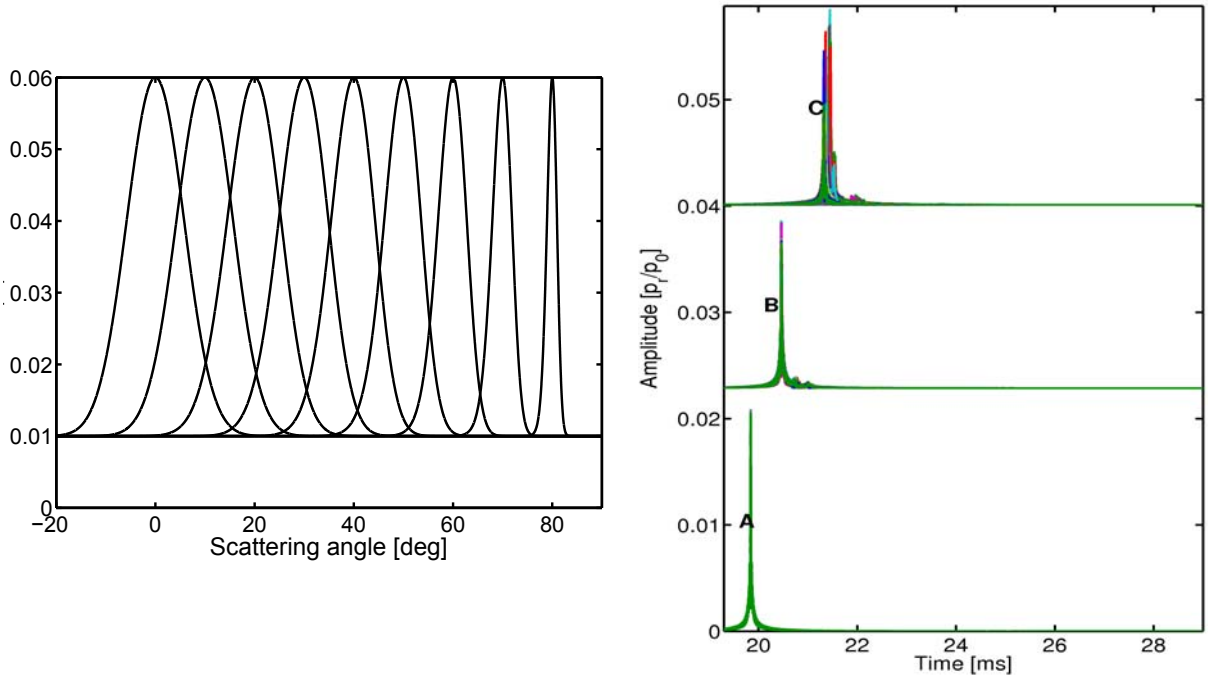

Figure 4: Left: Value of K from (19) for $R_{i0} = R_{r0} = 10$, $L = 0.5$, and, from left to right, for $\theta_{i0} = 0^{\text{o}}, -10^{\text{o}}, \cdots, -80^{\text{o}}$ and $\theta_{r0} = [-20^{\text{o}}, 90^{\text{o}}]$. Right: the simulation results corresponding to Figure 2 when this K is used to weight the facet components.

that when substituted with equations (11) in equation (15) and then in (12), gives

$$p_s(\mathbf{R_i}, \mathbf{R_r}) = \frac{p_0\left(\cos\theta_{r0} + \cos\theta_{i0}\right)}{2\sqrt{\left(\frac{\cos^2\theta_{r0}}{R_{r0}} + \frac{\cos^2\theta_{i0}}{R_{i0}}\right)\left(\frac{1}{R_{r0}} + \frac{1}{R_{i0}}\right)}} \frac{e^{ik_0(R_{i0}+R_{r0}-\frac{\alpha^2}{4U_x})} e^{\frac{-x_0^2}{2L^2}}}{R_{i0}R_{r0} + \gamma x_0}. \tag{17}$$

This is the equation we were looking for, because in the specular direction

$$\theta_{i0} = \theta_{r0},\ \cos\theta_{i0} = \cos\theta_{r0},\ \alpha = 0,\ x_0 = 0,$$

and it becomes

$$p_s(\mathbf{R_i}, \mathbf{R_r}) = \frac{e^{ik_0(R_{i0}+R_{r0})}}{R_{i0} + R_{r0}}, \tag{18}$$

i.e., the equation of the specular reflection. For angles near specular reflection, the equation (17) has a complex dependence on all the parameters, but is mainly influenced by

$$e^{\frac{-x_0^2}{2L^2}} = e^{\frac{-\alpha^2}{4U_x^2 L^2}},$$

that causes a forward "reflection" lobe whose amplitude depends on θ_{i0}, R_{i0} and R_{r0}. The lobe amplitude tends to zero for $R_{i0} \to \infty$ and $R_{r0} \to \infty$. Coming back to equation (9), in the PAR-TIME model case, we have to consider that the scattering of these surface realizations are calculated for $R_{i0} \to \infty$ and $R_{r0} \to \infty$, hence the specular region is very narrow and the effect of $\chi(\alpha)$ is already taken into account in the scattered values. Equation (17) is valid until it is greater than $\frac{1}{R_{i0}R_{r0}}$ since when it is lower the contribution from incoherent scattering is predominant. For easier integration and in analogy with [9], the next equation will be used to substitute $\frac{1}{R_{i0}R_{r0}}$ in the computation of the scattering amplitude:

$$K(\mathbf{R_i}, \mathbf{R_r}) = \frac{\left(\cos\theta_{r0} + \cos\theta_{i0}\right)}{2\sqrt{\left(\frac{\cos^2\theta_{r0}}{R_{r0}} + \frac{\cos^2\theta_{i0}}{R_{i0}}\right)\left(\frac{1}{R_{r0}} + \frac{1}{R_{i0}}\right)}} \frac{e^{\frac{-x_0^2}{2L^2}} e^{ik_0(R_{i0}+R_{r0}-\frac{\alpha^2}{4U_x})}}{R_{i0}R_{r0} + \gamma x_0} + \\ + \frac{1}{R_{i0}R_{r0}}. \tag{19}$$

Figure 4 shows on the left the value of K for $R_{i0} = R_{r0} = 10$, $L = 0.5$, and, from left to right, for $\theta_{i0} = 0^{\text{o}}, -10^{\text{o}}, \cdots, -80^{\text{o}}$ and $\theta_{r0} = [-20^{\text{o}}, 90^{\text{o}}]$.

4 RESULTS AND CONCLUSIONS

Figure 4 shows, on the right, the simulation results obtained when equation (19) is implemented in the PAR-TIME simulation to calculate a single scattering echo (B and C). The amplitudes of the echoes are in agreement with the experimental data. Later arrivals of small amplitude are still present in the simulations but at such a low level that their presence in the data could have been masked by background noise. These results show that, starting from the Helmoltz-Kirchhoff integral, it was possible to find the approximated interpolation for reflection and scattering regions. Using this equation, forward scattering simulation and data are in good agreement. Further work will be necessary to find the same approximation for higher order multiple scattering and for backscattering. The scattering amplitude in PAR-TIME is not calculated using a Kirchhoff approximation since the surface roughness is usually too big for this approximation to hold. The effect of the characteristic equation in (9) is implemented avoiding the averaging in 9 by using realizations and by using the angular dependency of equation (19) ($\rho_0 = K$).

ACKNOWLEDGEMENTS

Many thanks go to Kevin Le Page and Chris Harrison, for our fruitful discussions, to Peter Nielsen and Warren Fox, for reviewing this document, and to Peter Thorne as his PhD thesis contains useful suggestions to obtain the interpolation function K.

REFERENCES

1. G. Canepa, A. Tesei, V. Jaud, and O. Sertlek. PAR-TIME: Propagation And Reverberation TIME-domain model. In T. Akal, ed., *Proceeding of the 10th European Conference on Underwater Acoustics*, vol. 3, pp. 1416–1423, Istanbul, Turkey, 5–9 July 2010.
2. A. Tesei, G. Canepa, M. Zampolli, A. Bellettini, G. Parisi, and M. Paoli. High-frequency scattering from rough interfaces: measurements from MARES'08. In P. L. Nielsen, C. H. Harrison, and J.-C. L. Gac, eds., *Proceedings of Int. Sym. on Underwater Reverberation and Clutter*, Lerici, Italy, September 2008. NATO Underwater Research Centre.
3. A. Tesei, G. Canepa, and M. Zampolli. Measurements and modeling of high-frequency acoustic scattering by a rough seafloor and sea surface. In *Proceedings of the 3rd International Conference and Exhibition on Underwater Acoustic Measurements: Technologies and Results*, Nafplion, Greece, 21–26 June 2009.
4. C. Harrison, G. Canepa, and A. Tesei. An HF acoustic model of sound propagation and reverberation in the presence of rough boundaries. In T. Akal, ed., *Proceeding of the 10th European Conference on Underwater Acoustics*, vol. 3, pp. 1392–1397, Istanbul, Turkey, 5–9 July 2010.
5. G. Canepa, M. Zampolli, and A. Tesei. High-frequency scattering from rough interfaces: model-data comparison. In P. L. Nielsen, C. H. Harrison, and J.-C. L. Gac, eds., *Proceedings of Int. Sym. on Underwater Reverberation and Clutter*, Lerici, Italy, September 2008. NATO Underwater Research Centre.
6. G. Canepa. A strategy for speeding up acoustic models: a ray tracer example. In T. Akal, ed., *Proceeding of the 10th European Conference on Underwater Acoustics*, vol. 3, pp. 1392–1397, Istanbul, Turkey, 5–9 July 2010.
7. C. S. Clay and H. Medwin. *Acoustical oceanography: principles and applications*. John Wiley & sons, New York, 1977.
8. P. Beckmann and A. Spizzichino. *The scattering of electromagnetic waves from rough surfaces*. Pergamon Press, Oxfod, 1963.
9. P. D. Thorne. *Broadband studies of acoustic scattering from a model rough surface*. PhD thesis, University of Bath, 1982.
10. M. Born and E. Wolf. *Principles of optics*. Pergamon Press, Oxfod, 1965.

Document Data Sheet

Security Classification		Project No.
Document Serial No.	**Date of Issue**	**Total Pages**
CMRE-PR-2014-011	January 2014	9 pp.

Author(s)

Canepa, G., Tesei, A.

Title

A novel approach for a bistatic scattering calculation suitable for sonar performance model.

Abstract

One of the classical approaches to the calculation of the sound pressure scattered from a rough surface is to sum the contributions to the field from a set of small tiles that approximate the surface. If the tiles are smaller than the wavelength, or infinitesimal, the Kirchhoff's, the Small slope and small perturbation approximations can give good results. However, these approximations are computational intensive. In addition, if the tiles are larger than the wavelength these approximations cannot be applied. This work proposes a novel approach to accurately calculate the bistatic scattering from a rough surface approximated by tiles larger than the wavelength. The theory behind the calculations includes both specular and off-specular scattering components with their correct amplitude contributions. The results of the new approach are applied to a sonar performance model and compared with high frequency data. The model-data comparison demonstrates the validity of the theory.

Keywords

Issuing Organization

Science and Technology Organization
Centre for Maritime Research and Experimentation

Viale San Bartolomeo 400, 19126 La Spezia, Italy

[From N. America:
STO CMRE
Unit 31318, Box 19, APO AE 09613-1318]

Tel: +39 0187 527 361
Fax:+39 0187 527 700

E-mail: library@cmre.nato.int